Supporting Information

Anthracene-terminated self-assembled hole transporting monolayer for perovskite solar cells

Materials

Unless explicitly stated, all chemicals, reagents, and solvents employed in synthesized materials and fabricating PSCs were obtained from commercial suppliers in regent grade quality and utilized without additional purification. All reactions were conducted under a nitrogen atmosphere, employing standard Schlenk line techniques to ensure an inert and controlled environment. For the materials used for device fabrication, Lead (II) iodide (PbI_2) are purchased from TCI Corp. Formamidinium iodide (FAI), and Methylazanium iodide (MAI) are purchased from Greatcell Solar. The Cesium iodide (CsI), Methylazanium chloride (MACl) are purchased from Xi'an Polymer Light Technology Corp, China. BCP is purchased from Advanced Election Technology CO., Ltd, China. PEABr and PCBM are bought from Luminescence technology corp, China. All the dissolving and processing solvents including N, N-dimethylformamide (DMF), dimethyl sulfoxide (DMSO), chloroform, chlorobenzene (CB), isopropanol (IPA) are anhydrous and are purchased from Sigma-Aldrich, United States. Compound 1 is synthesed in our lab through conventional Suzuki-Miyaura reaction. 1,4-dibromobutane, tetrabuthylammonium bromide, dichloromethane, triethyl phosphite, bromotrimethylsilane were bought from Innochem, China.

Synthesis

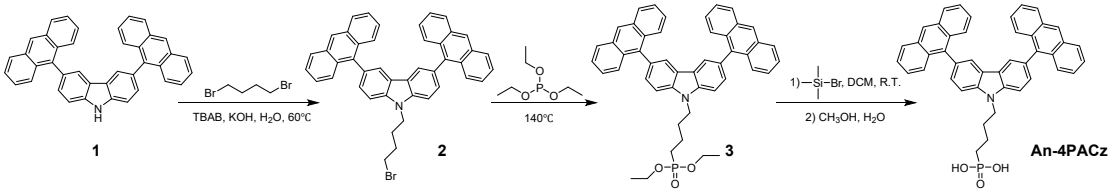

Scheme S1 Synthesis routine for An-4PACz.

Synthesis of compound 2

Compound 1 (compound 1, 1.0 mmol, 0.52 g), 1,4-dibromobutane (12 mmol, 0.26 g), tetrabuthylammonium bromide (0.2 mmol, 0.07 g) and 50% KOH aqueous solution (5 eq) were added into the flask. The reaction mixture was heated to 60 °C and kept stirring overnight under N_2. After cooling to R.T., the reaction mixture was extracted with dichloromethane. The organic layer was dried over anhydrous Na_2SO_4 and the solvent was distilled off under reduced pressure to give the crude product. The crude product was simply purified by short column chromatography (dichloromethane) to afford red solid (0.57 g, 87%).

Notes:

Compound 1 is completely reacted, as confirmed by TLC. A little by-product that another bromine on compound 2 is substituted by another Compound 1.

Due to the by-product would not react and is easier separated in the next step, therefore, we collect a mixture in the step. Due to the potential participate the reaction in the next

reaction, 1,4-dibromobutane is removed by column chromatography in this steps.

Synthesis of compound 3

compound 2 (0.87 mmol, 0.57 g) was dissolved in triethyl phosphite (20 eq, 17.6 mmol) and the reaction mixture was heated at 140 °C and keep stirring overnight under N_2. After reaction completion, the solvent was distilled off under reduced pressure. The crude product was purified by column chromatography (dichloromethane and ethyl acetate successively) to give yellow solid (0.53 g, 85%).

Notes: Column chromatography with dichloromethane as eluent could remove all the impurity, then ethyl acetate as the eluent to obtain compound 3.

Synthesis of An-4PACz

compound 3 (0.71 mmol, 0.53 g) was dissolved in anhydrous dichloromethane (10 mL) under N_2, then bromotrimethylsilane (10 eq) were added dropwise. The reaction mixture was stirred for overnight at R.T., then the solvent was distilled off under reduced pressure, the solid residue was reprecipitated. Afterwards, methanol (3 mL) was added and stirring for 3 h. Finally, distilled water was added dropwise (20 mL), until solution became opaque. Product was filtered off, dried to give yellow solid (0.45 g, 93%). ^{1}H NMR (600 MHz, DMSO) δ 8.64 (s, 2H), 8.22 (d, J = 1.3 Hz, 2H), 8.12 (d, J = 8.5 Hz, 4H), 7.95 (d, 2H), 7.61 (d, 4H), 7.48 (t, J = 7.6 Hz, 6H), 7.37 (d, J = 8.3, 4H), 4.65 (m, 2H), 2.10 (m, 2H), 1.82 - 1.68 (m, 4H). MALDI-TOF MS (*m/z*): $[M + H]^+$ calcd for $C_{44}H_{34}NO_3P$, 655.2276; found: 655.2267

Notes: All the obtained intermediates were used for the next step, and the overall yield from compound 1 is around 69%.

Details of computational calculation

Density functional theory (DFT) calculations were carried out using the QuantumATK simulation package.[1] Core electrons were treated with norm-conserving pseudopotentials from the SG15 library, combined with a medium basis set within the linear combination of atomic orbitals (LCAO) formalism. Structural optimizations of the investigated molecules were performed using the B3LYP hybrid exchange-correlation functional, with convergence achieved when the maximum atomic force fell below 0.01 eV/Å. A density mesh cutoff of 185 Ha was applied throughout the calculations. The HOMO–LUMO energy levels and corresponding orbital distributions are analyzed.

A 2×3 slab model of the PbI_2-terminated $FAPbI_3$ (001) surface was constructed from the optimized bulk structure, with a vacuum region of ~20 Å added along the surface normal to eliminate interactions between periodic images. Structural relaxations

were performed using a 3×3×1 Monkhorst-Pack k-point mesh and a plane-wave cutoff energy of 85 Ha. In this model, exchange–correlation interactions were described using the Perdew–Burke–Ernzerhof (PBE)[2] functional within the generalized gradient approximation (GGA) framework. Adsorption configurations of 4PACz and An-4PACz molecules were optimized on the perovskite surface, allowing full relaxation of all atoms in the molecules as well as the top two PbI_2–FAI bilayers. The adsorption energy (E_{ads}) was calculated to quantify the interaction strength between the adsorbate and the perovskite surface, using the following expression:
$E_{ads} = E_{\text{system}} - E_{substrate} - E_{adsorbate}$; where E_{system} is the total energy of the adsorbed system, $E_{substrate}$ is the energy of the pristine $FAPbI_3$ (001) surface, and $E_{adsorbate}$ is the energy of the isolated adsorbate molecule in vacuum.

Device fabrication process

The ITO (15 Ω) is cleaned with detergent, deionized water and ethanol for 15 minutes using the ultrasonic bath method. Before the deposition of SAMs, the substrate is processed with UV-Ozone for 10 minutes. The SAM film is prepared by spin-coating with 3000 r/m for 30 seconds in DMF solvent (0.5 mg mL^{-1}). After that, the film is heated at 100 °C for 10 minutes and washed with DMF. The perovskite precursor consisted of 1.6 M PbI_2, 1.4 M FAI, 0.07 M CsI, 0.07 M MAI, 0.2 M MACl, 1 mL DMSO and DMF solution with volume ratio of 8:2. The perovskite film is deposited by spin-coating with 1000 r/s for 10 seconds and 5000 r/s for 30 seconds. At the last 10 seconds, 150 μL of chlorobenzene solution was dropped on the perovskite. Then the film is annealed at 100 °C for 30 minutes. After cooled to room temperature, 1 mg mL^{-1} PEABr in IPA and DMF solvent (200:1) is deposited by spin-coating with 5000r/s and heated at 100 °C for 5 minutes. The PCBM (20 mg mL^{-1} in CB) is prepared by spin-coating with 1500 r/s for 30 seconds. After that, the BCP (0.5 mg mL^{-1} in IPA) is deposited with 5000 r/s for 30 seconds. Finally, Ag electrode with thickness of 120 nm was prepared by vacuum evaporation. The active area of the device was defined by a black mask with a size of 0.1225 cm^2 for all measurements.

Characterization

NMR spectra were recorded on a Brucker spectrometer (600 MHz). UV-vis spectra of investigated molecules are carried out on a UV-vis spectrophotometer (UV-3600 plus, Shimadzu Co. Ltd, Japan). The METATEST E3-300 contact angle tester was used to measure the moisture and precursor resistance of SAMs. The PL measurements of HTM were recorded on the fluorescence spectrophotometer (Hitachi F-4600, Japan). The PL spectrum of perovskite/HTM films were obtained from a fluorescence spectrometer (FLS980, Edinburgh, UK) with the excitation wavelength of 488 nm. The film morphology was measured by atomic force microscopy (5500AFM, Agilent Technologies, USA). The *J–V* characteristics were carried out using a Keithley 2400 source meter under AM 1.5G and a 3A grade solar simulator (Newport, USA) with an intensity of 100 mW cm^{-2}. The incident photon-to current conversion efficiency (IPCE) was recorded on QE/IPCE measurement kit (Sofn Instruments Co., LTD, China). The

wetting property of HTMs or perovskite precursor was measured on a contact angle tester (METATEST E3300). With a scan rate of 15°C min^{-1}, differential scanning calorimetry (DSC) is performed (METTLER-Toledo DSC1). SEM images were obtained by using a scanning electron microscope (SU8010 Hitachi).

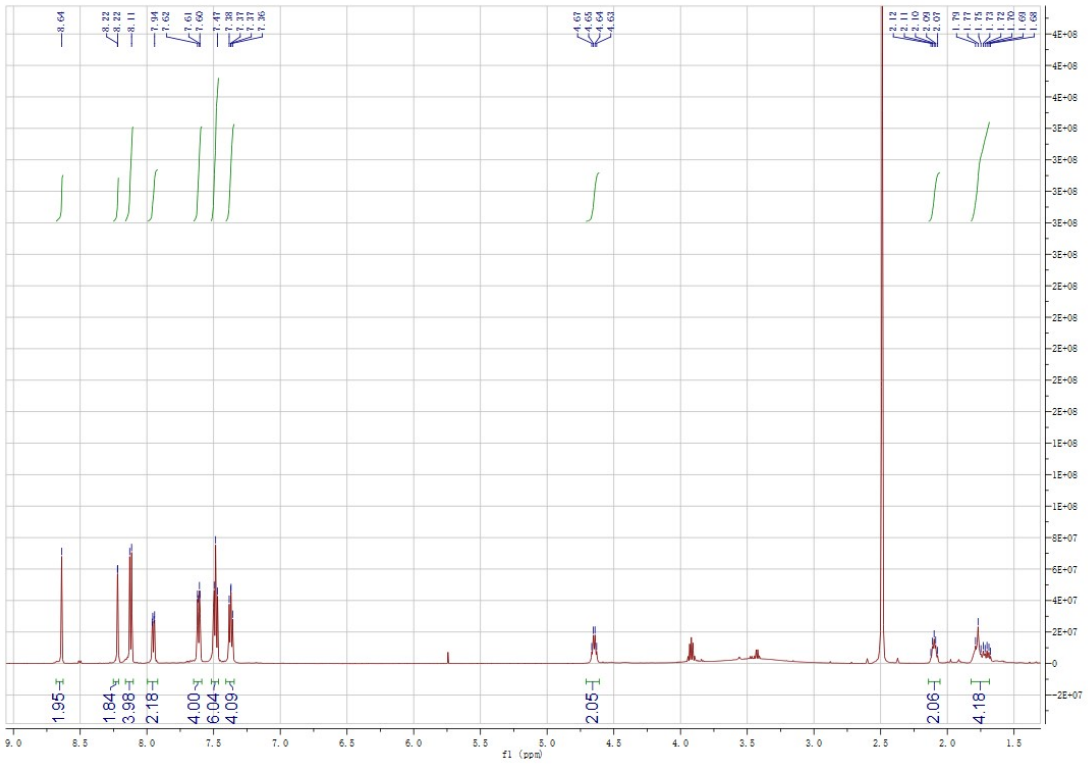

Fig. S1 ^{1}H NMR for An-4PACz.

Table S1 The dihedral angle between the carbazole and anthracene in An-4PACz.

	up	down
C1–C2–C3–C4 (right side)	-62.65°	-63.03
C1–C2–C3–C4 (left side)	50.91	46.06

C2–C3 is the bond connecting the carbazole and anthracene
C1 is in the carbazole ring adjacent to C2,
C4 is in the anthracene ring adjacent to C3.

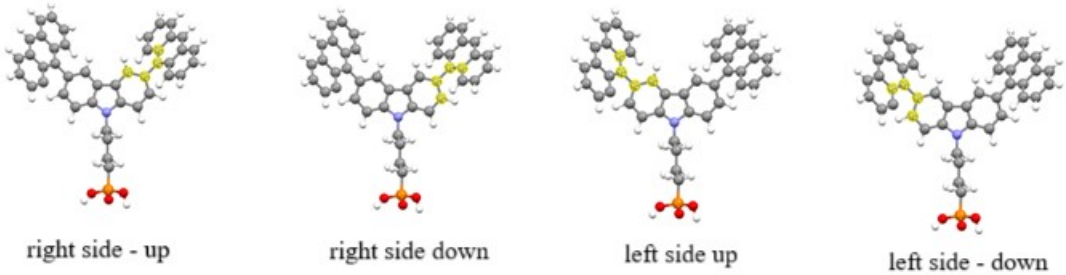

Fig. S2 Calculation schematic diagram

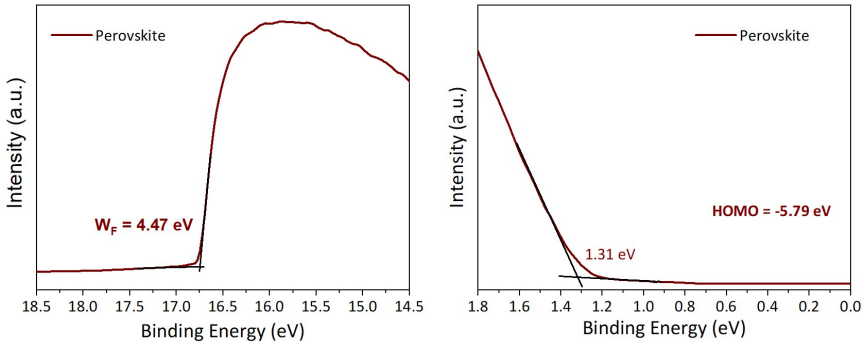

Fig. S3 The UPS image of perovskite.

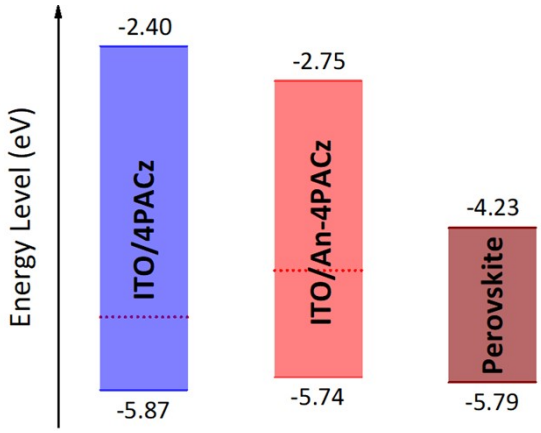

Fig. S4 Enengy level alignments of different SAMs and perovskite.

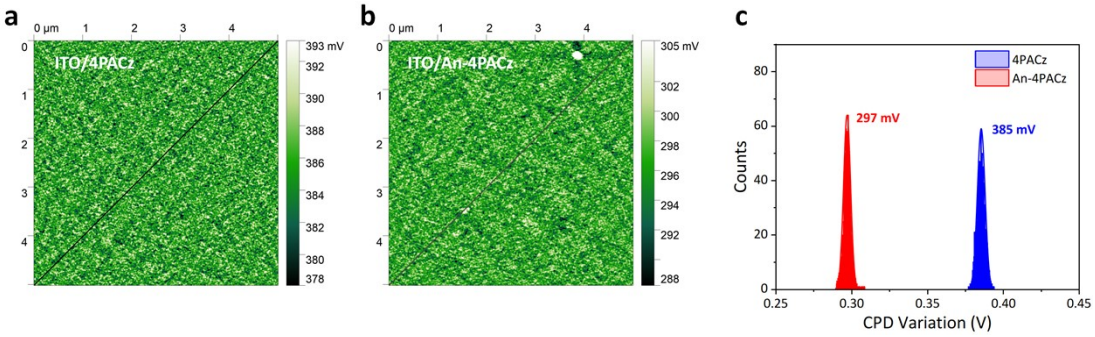

Fig. S5 The KPFM images of (a) 4PACz and (b) An-4PACz. (c) Statistical distribution of contact potential difference (CPD) extracted from corresponding KPFM images.

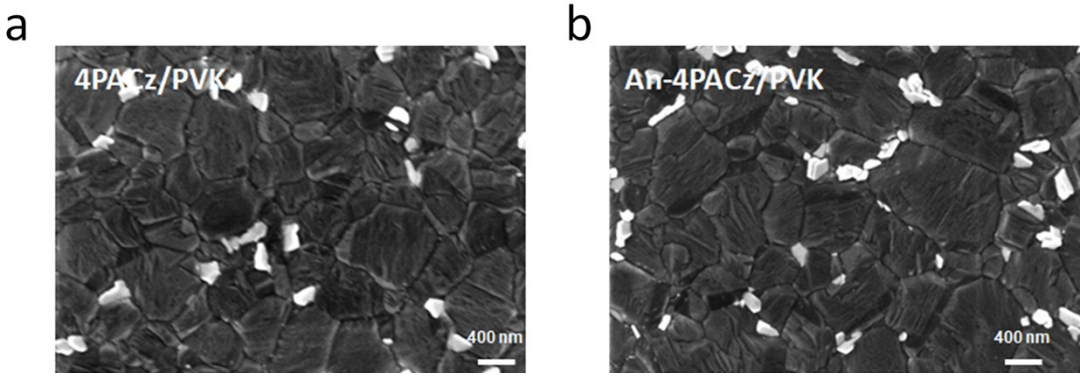

Fig. S6 Top-view SEM images of perovskite films deposited on (a) 4PACz and (b) An-4PACz.

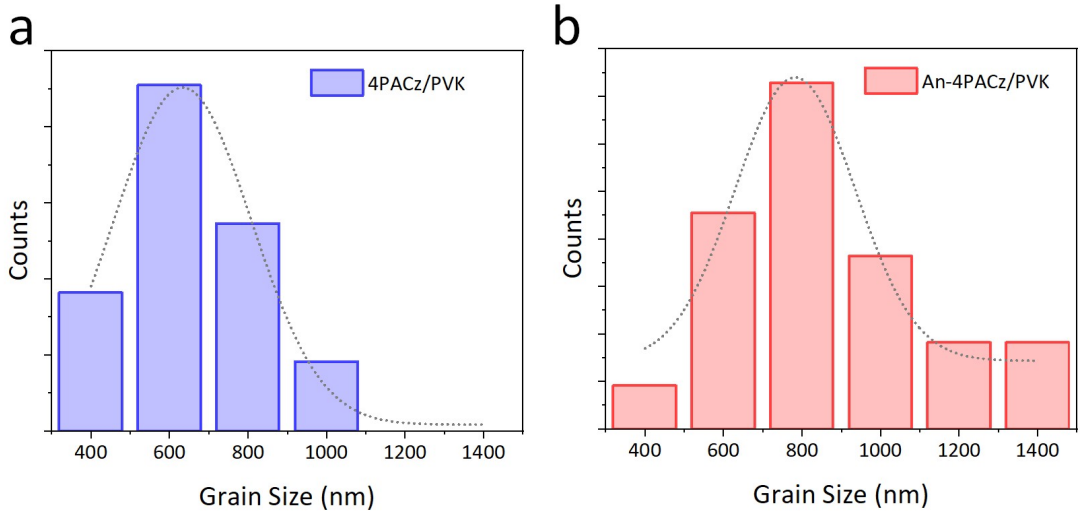

Fig. S7 The particle-size statistical distributions of perovskite films deposited on (a) 4PACz and (b) An-4PACz.

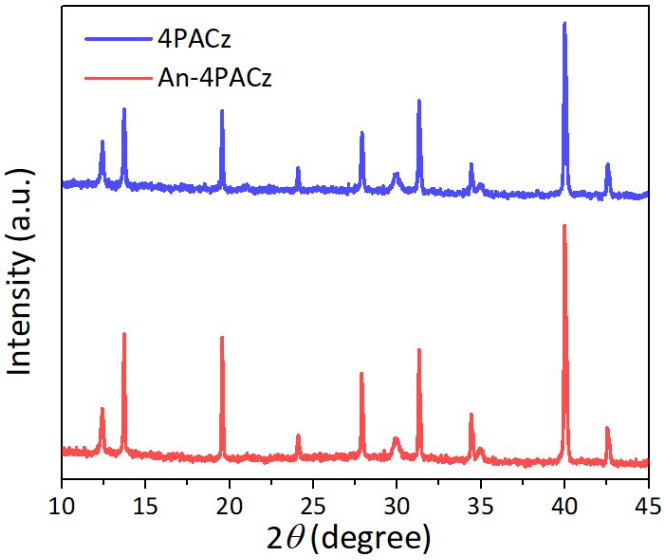

Fig. S8 XRD patterns of perovskite on different substrates.

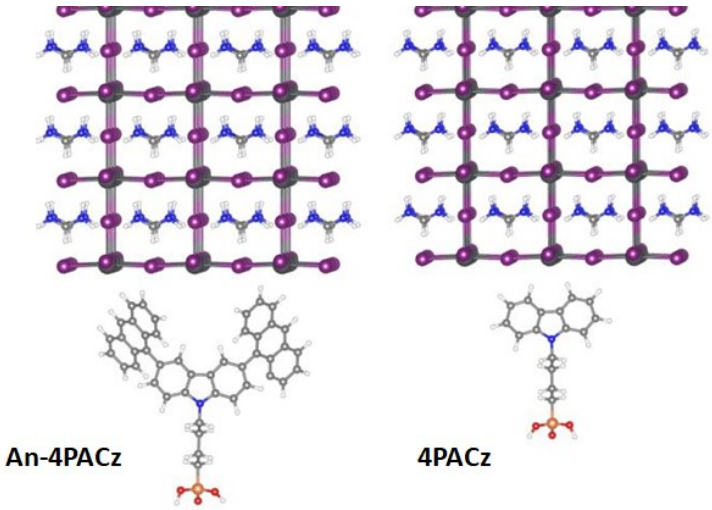

Fig. S9 Adsorption model of HTMs on the surface of the FAPbI3 layer An-4PACz and 4PACz.

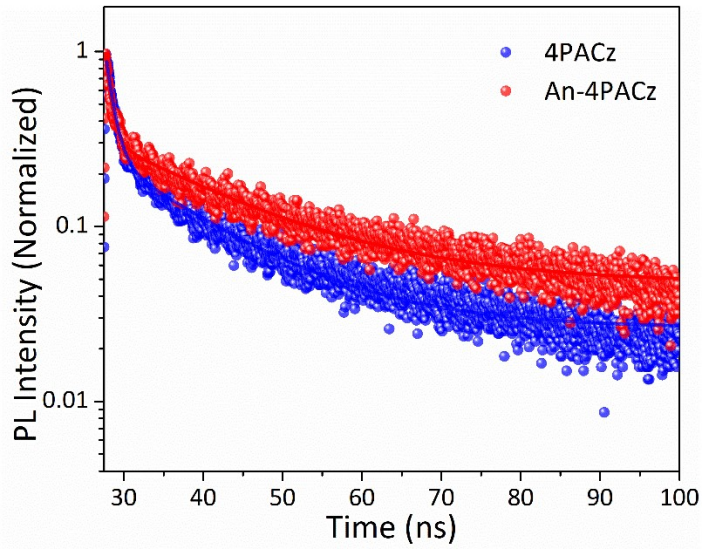

Fig. S10 TRPL curves of perovskite on different substrates.

Table S2 Fitted results of the TRPL spectra of perovskite film deposited on different substrates.

The TRPL decay spectra were fitted by a biexponential function:

$y = y_0 + a_1 e^{-(x-x0)/\tau 1} + a_2 e^{-(x-x0)/\tau 2}$

The average decay lifetime was calculated with function:

$A_1 = a_1\tau_1 / (a_1\tau_1 + a_2\tau_2)$

$A_2 = a_2\tau_2 / (a_1\tau_1 + a_2\tau_2)$

$\tau_{ave} = (a_1\tau_1^2 + a_2\tau_2^2) / (a_1\tau_1 + a_2\tau_2)$

SAM	A_1	τ_1 (ns)	A_2	τ_1 (ns)	τ_{ave} (ns)
An-4PACz	0.25	0.73	0.75	16.05	12.23
4PACz	0.36	0.97	0.64	12.80	8.58

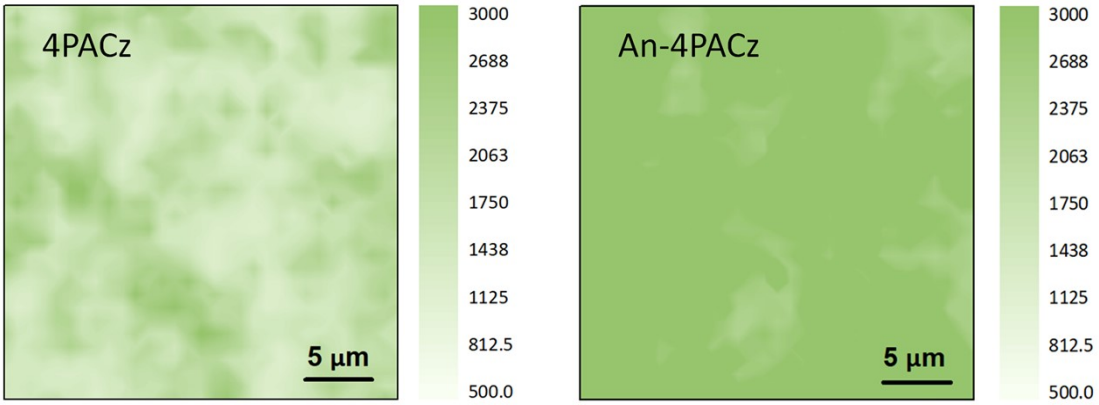

Fig. S11 PL mapping of perovskite on different substrates.

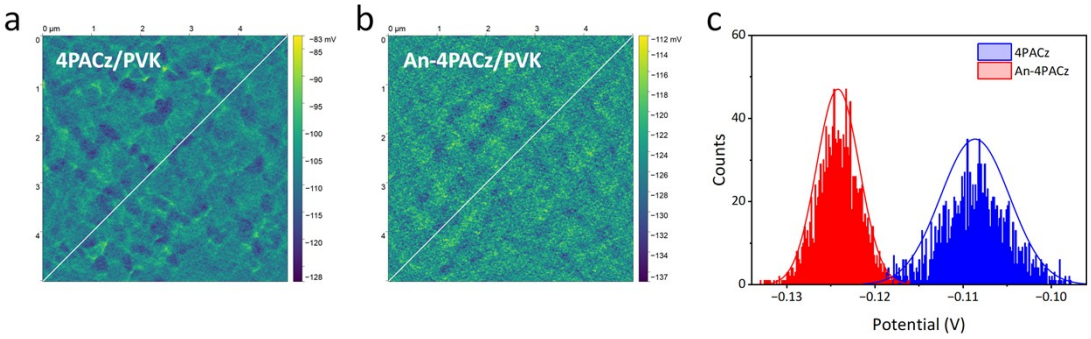

Fig. S12 KPFM measurement of (a) 4PACz and (b) An-4PACz coated on the ITO substrate. (c) Surface potential data of 4PACz and An-4PACz films extracted from KPFM.

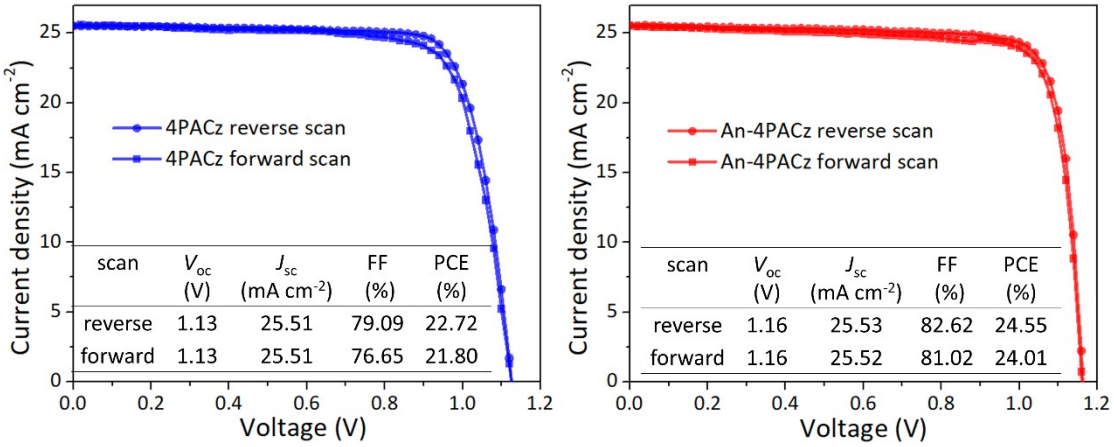

Fig. S13 Forward and reverse sweep *J-V* curves of the champion devices based on different SAMs.

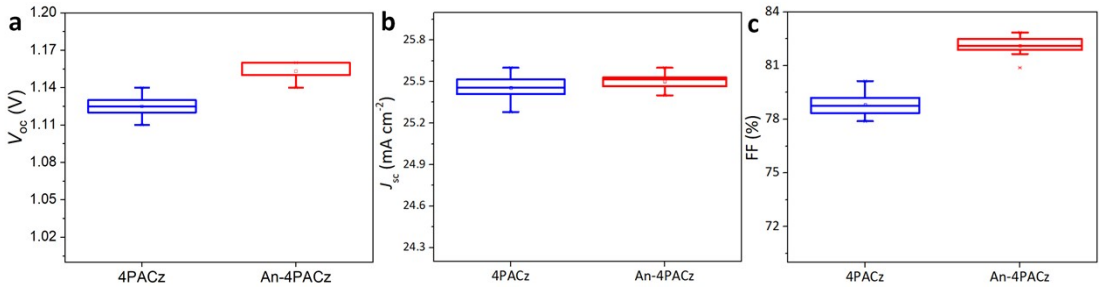

Fig. S14 Statistical distribution of the (a) V_{oc}, (b) J_{sc} and (c) FF.

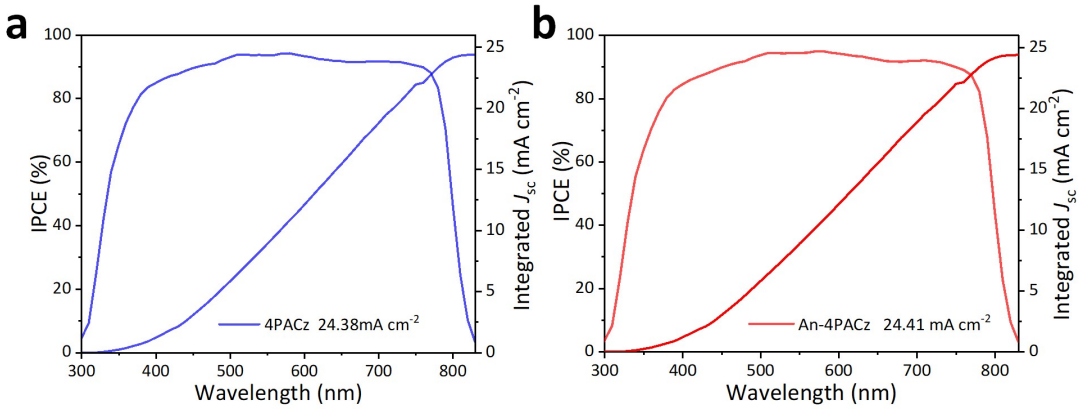

Fig. S15 IPCE spectra and integrated J_{sc} curve of (a) 4PACz and (b) An-4PACz based PSCs.

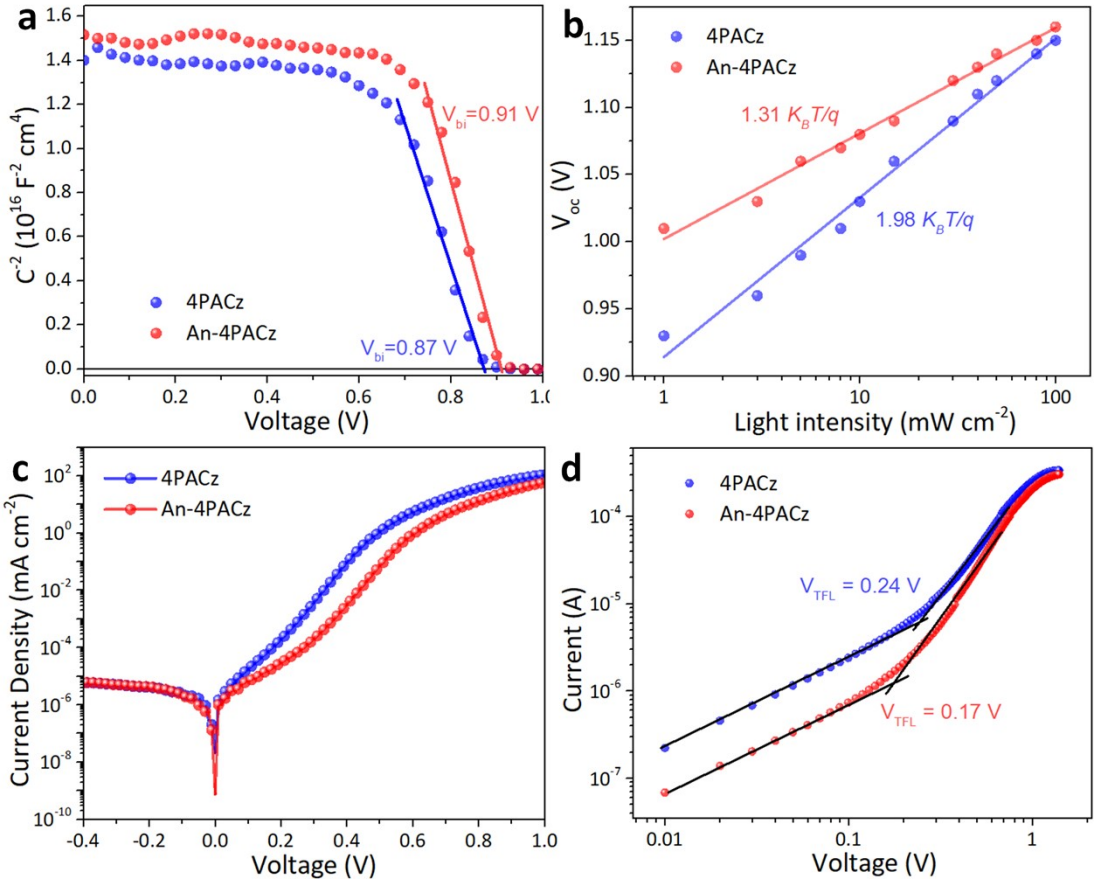

Fig. S16 (a) Mott–Schottky plots of PSCs, (b) V_{oc} dependency of the devices on the light intensity, (c) *J-V* curves under dark conditions, (d) SCLC curves of PSCs.

Reference

1. S. Smidstrup, T. Markussen, P. Vancraeyveld, J. Wellendorff, J. Schneider, T. Gunst, B. Verstichel, D. Stradi, P. A. Khomyakov, U. G. Vej-Hansen, M.-E. Lee, S. T. Chill, F. Rasmussen, G. Penazzi, F. Corsetti, A. Ojanperä, K. Jensen, M. L. N. Palsgaard, U. Martinez, A. Blom, M. Brandbyge and K. Stokbro, *J. Phys. Condens. Matter*, 2019, **32**, 015901.
2. J. P. Perdew, K. Burke and M. Ernzerhof, *Phys. Rev. Lett.*, 1996, **77**, 3865.